

Effect of sheet thickness on the microstructural evolution of an Mg AZ61 alloy during large strain hot rolling

M.T. Pérez-Prado^{*}, J.A. del Valle¹, O.A. Ruano

Department of Physical Metallurgy, Centro Nacional de Investigaciones Metalúrgicas (CENIM), CSIC, Avda. Gregorio del Amo, 8, 28040 Madrid, Spain

Received 30 April 2003; received in revised form 30 April 2003; accepted 11 November 2003

Abstract

Using texture analysis and optical microscopy it has been found that, due to the large anisotropy of the hcp lattice, the deformation mechanism predominant during large strain hot rolling of an AZ61 Mg alloy changes from dislocation slip and rotational recrystallization (RRX) to twinning as the sheet thickness is reduced.

© 2003 Acta Materialia Inc. Published by Elsevier Ltd. All rights reserved.

Keywords: Magnesium; Large strain hot rolling; Texture; Microstructure; Twinning

1. Introduction

Research in Mg alloys has surged in recent years due to the excellent specific properties of these materials. Significant efforts have been devoted to investigate and model the microscopic mechanisms predominant during different thermomechanical processing routes in order to optimize microstructural design of Mg alloys for different applications [1–7]. Owing to their high anisotropy, hcp metals show a complex deformation behavior. The lack of slip systems and their asymmetric distribution causes other deformation mechanisms such as twinning to operate to different extents depending on the deformation conditions [3]. Still further work is needed in this area since, for example, the evolution of texture and microstructure in hcp materials during simple processes such as hot rolling is still not thoroughly understood.

In a former paper [8] the present authors described a thermomechanical processing route consisting of only two to three rolling passes of large thickness reduction per pass (large strain hot rolling, LSHR), that allowed significant grain refinement in an AZ61 alloy with an initial strong basal texture. The final grain size achieved was in the micron scale. The resulting microstructure

proved to have excellent superplastic properties at intermediate to low temperatures. The effect of alloy composition, texture, or sheet thickness/roll diameter ratio on the microstructural evolution during LSHR of Mg alloys has still not been systematically studied. In the present paper the influence of the initial sheet thickness on the deformation mechanisms and microstructure developed during LSHR of an AZ61 alloy is investigated.

2. Experimental procedure

The material used for this investigation is an Mg AZ61 alloy extruded in the form of a 10-mm-thick sheet. The main alloying elements of this material are Al (6%) and Zn (1%).

Slabs of two different thicknesses (4 and 1 mm) were cut out of the initial sheet. Both the as-received sheet and the two slabs were subjected to one rolling pass of 30% reduction at 375 °C (a larger thickness reduction in the first pass caused cracking, although larger reductions can be imposed in the second pass [8]). After rolling samples were quenched in water. The microstructural evolution during LSHR of the 10-mm-thick sheet was described in [8] and is also briefly reported in this paper for comparison with the 4- and 1-mm-thick sheets.

The microstructure of the rolled samples was examined by optical (OM) and scanning electron microscopy

^{*} Corresponding author. Tel.: +34-91-553-8900; fax: +34-91-534-7425.

E-mail address: tprado@cenim.csic.es (M.T. Pérez-Prado).

¹ On leave from CONICET, Argentina.

(SEM). Sample preparation for OM and SEM consisted on grinding on SiC paper with increasingly finer grits, followed by mechanical polishing with 6 and 1 μm diamond paste and final polishing using colloidal silica. Additionally, for OM the grain structure was revealed by subsequent etching using a solution of ethanol (100 ml), picric acid (5 g), acetic acid (5 ml) and water (10 ml). After chemical etching a residual layer remained in the sample surface that was eliminated by immersion in boiling ethanol. True grain sizes were measured by the linear intercept method using a correction factor of 1.74. X-ray texture analysis was carried out in all the rolled samples using the Schulz reflection method in a Siemens D5000 diffractometer furnished with a closed Eulerian cradle. Sample preparation for texture analysis was done in the same way as for SEM.

3. Results

Fig. 1 shows the microstructure (Fig. 1a) and texture (Fig. 1b) of the AZ61 alloy in the as-received condition. The optical micrograph in Fig. 1a shows an equiaxed microstructure with an average grain size of about 54 μm [8]. The texture is represented in Fig. 1b by means of the (0002) (basal) pole figure. It can be seen that the texture is formed by a strong basal fiber component (i.e., a large volume fraction of grains are oriented with basal planes parallel to the rolling plane) as well as a weak prismatic component (i.e., a few grains with prismatic planes parallel to the rolling plane are also present).

The microstructures corresponding to the three rolled sheets after a pass of 30% reduction at 375 $^{\circ}\text{C}$ are shown in Fig. 2a–e, respectively. The micrographs were taken in the mid-thickness both along the rolling plane (RP) (Fig. 2a–c) and along the plane formed by the rolling (RD) and normal (ND) directions (RN plane) (Fig. 2d–f). As can be seen in Fig. 2a, significant grain refinement

takes place in the 10-mm-thick sheet after rolling. Grain size is rather homogeneous, although still some large initial grains remain present. The average grain size decreases down to 11.4 μm . Only a few twins could be observed. The microstructural evolution of the 4-mm-thick sheet is rather different, as can be seen in Fig. 2b. Recrystallized small grains are apparent along grain boundaries and twinned regions (see arrows in Fig. 2b), as previously observed in an AZ31 alloy [7], and therefore a sharply bimodal grain size distribution develops. The average grain size of the small grains is 2.8 μm . The larger grains are about 53 μm in size. The volume fraction of twinned material increases significantly with respect to the 10-mm-thick sheet. Finally, in the 1-mm-thick sheet (Fig. 2c and f) no grain size reduction is observed. Instead, extensive twinning takes place in all the grains. SEM examination revealed that a large fraction of narrow twins form, most of which are as thin as 100–200 nm in width.

A close look at the transverse sections (RN planes), illustrated in Fig. 2d–f, reveals that *banding* takes place in the three sheets in order to accommodate the imposed deformation. Thus, *bands* at 35–45 $^{\circ}$ angles with respect to the RD develop. This effect is more pronounced in the 4- and 1-mm-thick sheets. The mechanism for band formation is different for each sheet thickness. In the 10-mm sheet, the bands are formed by the refined recrystallized grains [8]. In the 4-mm sheet, they consist of the small grains apparent at the grain boundaries and twinned regions. Finally, in the 1-mm sheet, the bands are constituted by the narrow twins developed. It can be seen that twin bands traverse grain boundaries.

Fig. 3 illustrates the texture of the rolled sheets by means of the (0002) pole figures. This representation was considered the most adequate because, in all cases, no new texture components appear after deformation. However, important changes in the intensity of the basal fiber texture can be appreciated. A significant intensity

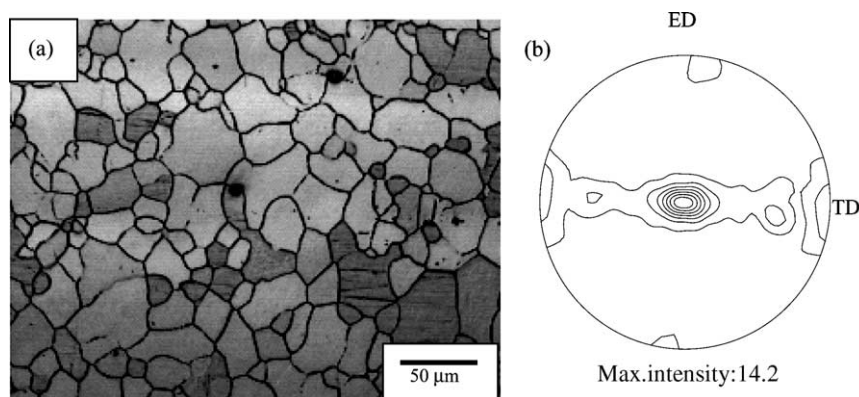


Fig. 1. Microstructure of the as-received AZ61 alloy. (a) Optical micrograph; (b) (0002) X-ray pole figure. Levels: 1, 3, 5, 7, 9, 11, 13. The sheet normal is in the center of the pole figure. The extrusion direction (ED) is the vertical direction. The transverse direction (TD) is the horizontal direction.

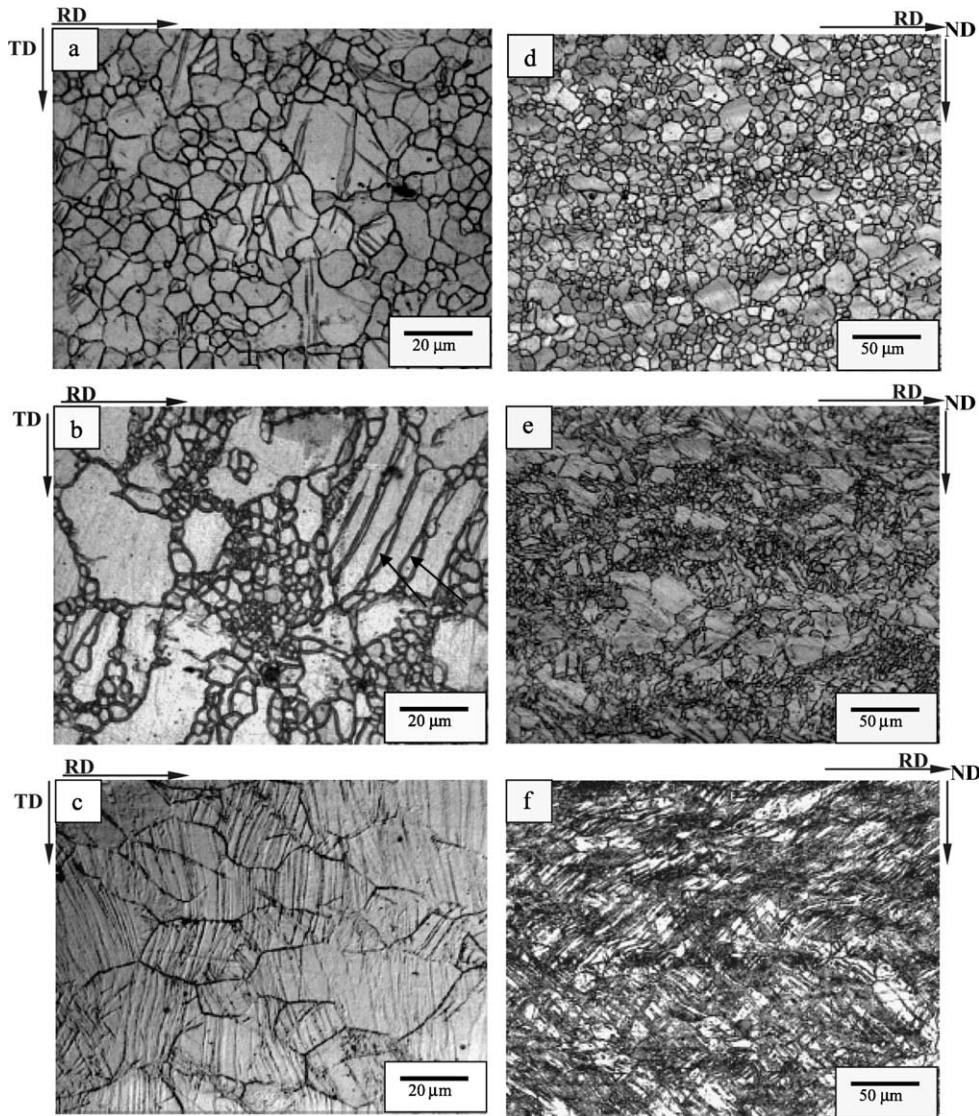


Fig. 2. Microstructure of the rolled AZ61 alloy. (a) RP: 10 mm thickness sheet; (b) RP: 4 mm thickness sheet; (c) RP: 1 mm thickness sheet; (d) RN plane: 10 mm thickness sheet; (e) RN plane: 4 mm thickness sheet; (f) RN plane: 1 mm thickness sheet. The rolling direction in all cases is the horizontal. In (c) the arrows point towards recrystallized grains located at twin boundaries.

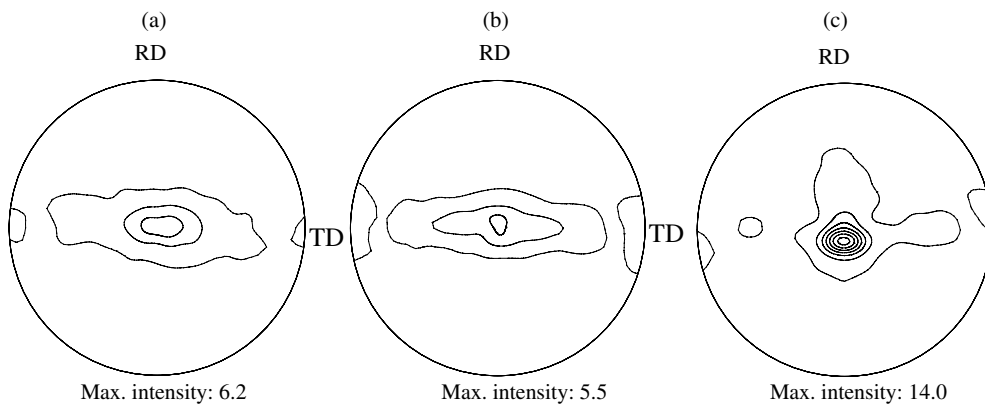


Fig. 3. Macrotexture of the rolled samples illustrated using the (0002) pole figure: (a) 10-mm-thick sheet; (b) 4-mm-thick sheet; (c) 1-mm-thick sheet. Levels: 1, 3, 5, 7, 9, 11, 13.

decrease and a spread in the basal pole towards the transverse direction (TD) is apparent after rolling the 10- and 4-mm-thick sheets. In the 1-mm-thick sheet, however, the texture intensity is similar to that of the as-received material and no texture spread is observed. It should be noted that the prismatic component disappears in all cases, probably due to twinning of prismatic grains in the $\{11-20\}$ system, which would bring the basal planes into alignment with the rolling plane [4].

4. Discussion

The results described above evidence that the microstructural evolution during large strain hot rolling of an AZ61 Mg sheet with an initial strong basal texture is highly dependent on the initial thickness for a given rolling temperature and reduction per pass. This also substantiates the complexity of deformation in hcp polycrystals. In general, a variation in the sheet thickness has the effect of changing the angle between the sheet ND and the radial force,

$$\cos \theta = \frac{R - \frac{h_0 - h_f}{2}}{R}, \quad (1)$$

where R is the roll radius ($=65$ mm), h_0 is the initial sheet thickness, h_f is the final thickness, and θ is the angle between the ND and the radial force (P_r), see Fig. 4 [9]. The θ angles corresponding to the 10-, 4-, and 1-mm-thick sheets are, respectively, 12.3° , 7.8° , and 3.9° . These small angle variations are enough to change the predominant deformation mechanism during rolling of the AZ61 alloy.

Fig. 5 shows the so-called “fiber plot” corresponding to the as-received AZ61 alloy, i.e., a 2D representation of the density of orientations ($f(\lambda)$) vs. the angle between their c -axis and the ND (λ). This fiber plot has been calculated from the X-ray pole figure by a procedure described in [10]. The representation of the density of orientations vs. the angle between their c -axis and P_r for each sheet thickness would thus be $f(\lambda - \theta)$. Therefore the origin of the “fiber plot” (taken as the

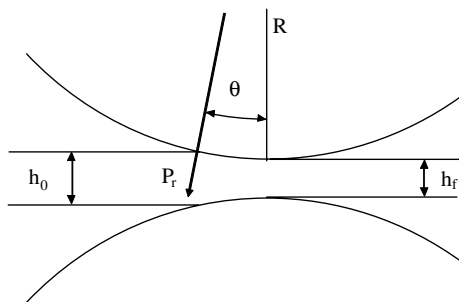


Fig. 4. Schematic showing the direction of the radial force as a function of the sheet thickness and the roll radius.

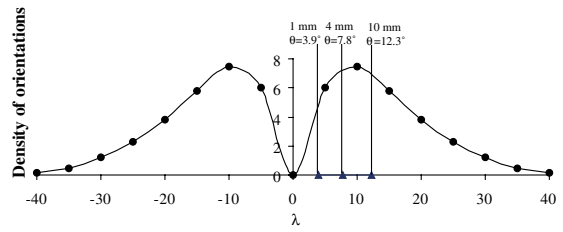


Fig. 5. 2D fiber plot showing the density of orientations with c -axes forming an angle λ with the ND. The lines indicate the origin of the plot $f(\lambda - \theta)$ corresponding to each initial sheet thickness.

direction of the radial force in each case, i.e., $\lambda - \theta = 0$) shifts with increasing θ as illustrated in Fig. 5.

In the 1-mm-thick sheet, the majority of the c -axis form angles smaller than 25° with respect to the radial force and there is only a small volume fraction of grains with c -axis parallel to P_r . In this situation, the Schmid factors for both basal and prismatic planes are low [3], and twinning is favored in spite of the fact that twinning usually becomes less important at high temperatures. The retention of the basal fiber texture suggests that a double twinning mechanism may take place [3]. First, twinning on the $\{11-22\}$ system would rotate the c -axes away from the sheet normal by about 64° . Second, twinning on the $\{10-12\}$ system would bring back the c -axes almost into alignment with the direction of the applied stress, i.e., into better alignment with the ND than they were before deformation. The absence of zones of localized deformation along grain boundaries suggests that the activated twinning systems allow intergranular strain compatibility.

In the 10-mm-thick sheet, the significant decrease in the intensity of the basal texture and the small fraction of twinned material suggest that deformation takes place mainly by dislocation slip. This is consistent with the fact that, first, a rather large number of grains have c -axes forming high angles (as high as $40-45^\circ$) with respect to the radial force (type-A grains) and second, a significant number of grains have c -axes aligned (or forming small angles) with P_r (type-B grains) (see Fig. 5). In type-A grains both basal and non-basal slip systems have rather high Schmid factors and low CRSS and thus may be activated. As a consequence of slip, grains may rotate to stable positions under the imposed stress. Grain refinement in these grains may take place by continuous dynamic recrystallization (CDX) [11], a process that occurs readily in Mg alloys [12,13]. Type-B grains are not able to accommodate the imposed deformation by dislocation slip in both basal and prismatic planes, which have Schmid factors close to 0. Twinning could constitute an alternative deformation mechanism in these grains, but significant twinning is not observed. Instead, type-B grains accommodate the imposed deformation by rotational recrystallization (RRX). This process, which was described in detail in

[8], occurs as a result of stress concentrations along grain boundaries due to strain incompatibilities in neighbouring grains [14]. The appearance of these stresses is consistent with the availability of an insufficient number of deformation modes. Thus, RRX would give rise to rotation of the “mantle” regions (areas along the boundaries where the stress is higher than that of the grain core is present) away from the orientation of the original grain into orientations more favorable for slip [15]. This is consistent with the decrease of the basal texture intensity. The spread of the basal poles towards the TD is associated with the operation of non-basal slip and it has been previously observed in Mg–Li alloys and in Zr and Ti alloys [3,4,16], where prismatic slip predominates.

The 4-mm-thick sheet is an intermediate case. Both twinning and slip act as deformation modes to some extent and thus the stress due to plastic incompatibility at the grain boundaries decreases. Therefore the “mantle” region extends to smaller distances within the grains [17] and smaller grains are formed by RRX. Additionally, regions of small grains resulting from CDX in grains originally oriented more favorably for slip (similar to type-A grains) can also be clearly seen (see clustering of small grains in Fig. 2c). All the above observations are consistent with the decrease in the intensity of the basal fiber texture after rolling. Once again, the spread of basal poles towards the TD suggests the importance of non-basal slip.

5. Conclusions

The effect of the initial sheet thickness on the microstructural evolution during large strain hot rolling of an AZ61 Mg alloy sheet has been investigated using OM and texture analysis as the main characterization tools. It has been found that significant changes in the predominant deformation mechanisms occur as a consequence of the increase in the angle between the radial force and the sheet normal (ND) with increasing sheet thickness. Double twinning predominates in the thinnest sheet, and RRX and dislocation slip become increas-

ingly more important as thickness increases, leading ultimately to significant grain refinement. In particular, non-basal slip seems to play an important role during deformation of the sheets with larger thickness.

Acknowledgements

The authors acknowledge financial support from CICYT grant MAT2000-1313 as well as from a Ramón y Cajal contract. JAV acknowledges support from a postdoctoral grant from CONICET, Argentina.

References

- [1] Katrak FE, Agarwal JC, Brown FC, Loreth M, Chin DL. In: Kaplan HI, Hryn J, Clow B, editors. Magnesium technology 2000. The Minerals, Metals and Materials Society; 2000. p. 351.
- [2] Philippe MJ. Mater Sci Forum 1994;157–162:1337.
- [3] Tenckhoff E. Deformation mechanisms, texture, and anisotropy in zirconium and zircalloy. ASTM STP 1988;966:45.
- [4] Roberts CS. Magnesium and its alloys. New York: John Wiley & Sons; 1960. p. 190.
- [5] Bakarian PW. Trans AIME 1941;147:266.
- [6] Agnew SR, Yoo MH, Tomé CN. Acta Mater 2001;49:4277.
- [7] Myshlyayev MM, McQueen HJ, Mwembela A, Konopleva E. Mater Sci Eng A 2002;337:121.
- [8] Del Valle JA, Pérez-Prado MT, Ruano OA. Mater Sci Eng A 2003;355:68.
- [9] Dieter GE. Mechanical metallurgy. New York: McGraw-Hill; 1986. p. 586.
- [10] Borrego A, Fernández R, Cristina MC, Ibáñez J, González-Doncel G. Comp Sci Tech 2002;62:731.
- [11] Doherty RD, Hughes DA, Humphreys FJ, Jonas JJ, Juul Jensen D, Kassner ME, et al. Mater Sci Eng A 1997;238:219.
- [12] Galiyev AM, Kaibyshev RO, Gottstein G. In: Gottstein G, Molodov DA, editors. Proceedings of the First Joint International Conference on Recrystallization and Grain Growth. New York: Springer-Verlag; 2001. p. 893.
- [13] Gourdet S, Montheillet F. Mater Sci Eng A 2000;283:274.
- [14] Koike J, Kobayashi T, Mukai T, Watanabe H, Suzuki M, Maruyama K, et al. Acta Mater 2003;51:2051.
- [15] Ion SE, Humphreys FJ, White SH. Acta Metall 1982;30:1909.
- [16] Agnew SR, Yoo MH. In: Kaplan HI, Hryn J, Clow B, editors. Magnesium technology 2000. The Minerals, Metals and Materials Society; 2000. p. 331.
- [17] Margolin H, Stanescu MS. Acta Mater 1975;23:1411.